

**The Katzman Automatic Imaging Telescope Gamma-Ray Burst
Alert System, and Observations of GRB 020813**

Weidong Li, Alexei V. Filippenko, Ryan Chornock, Saurabh Jha

Email: (wli, alex, rchornock,sjha)@astro.berkeley.edu

Department of Astronomy, University of California, Berkeley, CA 94720-3411

Received _____; accepted _____

Submitted to PASP

ABSTRACT

We present the technical details of the gamma-ray burst (GRB) alert system of the Katzman Automatic Imaging Telescope (KAIT) at Lick Observatory, and the successful observations of the GRB 020813 optical afterglow with this system. KAIT responds to GRB alerts robotically, interrupts its pre-arranged program, and takes a sequence of images for each GRB alert. A grid-imaging procedure is used to increase the efficiency of the early-time observations. Different sequences of images have been developed for different types of GRB alerts. With relatively fast telescope slew and CCD readout speed, KAIT can typically complete the first observation within 60 s after receiving a GRB alert, reaching a limiting magnitude of ~ 19 .

Our reduction of the GRB 020813 data taken with KAIT shows that unfiltered magnitudes can be reliably transformed to a standard passband with a precision of $\sim 5\%$, given that the color of the object is known. The GRB 020813 optical afterglow has an exceptionally slow early-time power-law decay index, though other light-curve parameters and the optical spectral index are fairly typical of GRBs.

Subject headings: gamma rays: bursts – telescopes – instrumentation:
miscellaneous

1. INTRODUCTION

Although the study of gamma-ray bursts (GRBs) has been revolutionized in the past few years because of the successful operation of several space GRB detection experiments [such as the Burst and Transient Source Experiment (BATSE) on board the Compton Gamma Ray Observatory (CGRO), Meegan et al. 1992; the BeppoSAX satellite, Boella et al. 1997; and the High Energy Transient Explorer-2 (HETE-2), Ricker et al. 2001], the origin and nature of GRBs remain enigmatic. Much of the difficulty in studying GRBs results from their short duration ($\sim 1\text{--}100$ s), the generally poor precision of their reported positions, and the rapidly fading brightness of their counterparts in the lower-energy passbands (X-ray, optical, and radio). Since the detection and observation in these lower-energy passbands during and shortly after a GRB potentially holds the key to significant progress in understanding the central engine of GRBs and could provide valuable clues to their progenitors (Mészáros 2001), it is critical to have nearly real-time position determination and prompt follow-up observations in all passbands shortly after the trigger of a GRB.

HETE-2 is currently the only GRB detector capable of localizing and disseminating GRB positions in nearly real-time, and the GRB Coordinates Network (GCN; Barthelmy et al. 1994) provides a link between GRB triggers and observers/telescopes, including real-time distribution of GRB alerts to a handful of sites with robotic equipment. The successful observation of the GRB 990123 optical afterglow (OA) by the Robotic Optical Transient Search Experiment (ROTSE; Akerlof & McKay 1999; Akerlof et al. 1999) only 22 s after the GRB trigger, and observations by the Livermore Optical Transient Imaging System (LOTIS) and Super-LOTIS (Park et al. 2001), demonstrate that it is useful to have robotic telescopes that can respond to GRB alerts automatically.

In this paper we describe the GRB alert system with the 0.76 m (30 inch) Katzman Automatic Imaging Telescope (KAIT), currently the world’s largest robotic telescope capable of responding to GRB alerts and doing real-time GRB optical follow-ups. KAIT can reach a limiting magnitude of ~ 19 in a 20 s unfiltered exposure, and can slew at a

relatively fast speed (5° s^{-1}). The main goal of the KAIT GRB alert system is not to search widely for OAs of GRBs, as KAIT’s ability to detect a particular GRB OA is limited by its small field of view ($6'.7 \times 6'.7$), but rather to obtain a high-quality early-time light curve of a GRB OA once it is detected in the KAIT field. With these early-time data we will be able to constrain properties of GRBs such as (1) the temporal behavior of the OA emission, (2) breaks and undulations in the light curves, and (3) other derived parameters such as the initial Lorentz factor of the blast wave, the jet opening angle, and the ambient medium density. The relatively deep, rapid observations made by KAIT will also provide useful constraints on some of the well-localized “dark GRBs,” in which no optical afterglow is seen. The best example to date of KAIT’s abilities was provided by KAIT observations of GRB 021211 (Li et al. 2003), which showed evidence of reverse shock emission at early times.

The paper is organized as follows. Section 2 contains a description of KAIT, the GRB alert system, and the performance of the system in its first year of operation. Section 3 reports the successful observations of the GRB 020813 OA with this system, and the transformation of the observed unfiltered photometry to a standard system. Conclusions are drawn in Section 4.

2. THE KAIT GRB ALERT SYSTEM

2.1. KAIT

KAIT is the third robotic telescope in the Berkeley Automatic Imaging Telescope (BAIT) program. The technical details, the operation concept, and the scientific objectives of the earlier BAIT systems can be found in Filippenko (1992), Richmond, Treffers, & Filippenko (1993), and Treffers et al. (1995), while those of KAIT specifically are in Li et al. (2000), Filippenko et al. (2001), and Filippenko et al. (2003, in preparation). Here we briefly summarize the operation concept of KAIT and the results from the ongoing supernova (SN) search.

KAIT consists of a 0.76 m diameter primary with a Ritchey-Chretien mirror set. The telescope has a focal ratio of $f/8.2$ and a plate scale of $33''.2 \text{ mm}^{-1}$ at the focal plane. An off-axis autoguider enables long exposure times. The thermoelectrically cooled CCD camera is an Apogee AP7b with a SITe 512×512 pixel back-illuminated chip (pixel size $24 \mu\text{m}$), which has a pixel scale of $0''.8$. We use only the central 500×500 pixels in observations due to some chip defects near the edges, yielding a total field of view (FOV) of $6''.7 \times 6''.7$. KAIT has a filter wheel with 20 slots, including a set of standard Johnson UBV and Cousins RI filters. A weather station monitors the outside and telescope temperatures, humidity, wind speed, rain, and cloud cover, and it sends signals to close the dome slit whenever conditions are hazardous to the telescope system.

All of the hardware is controlled by computers. The whole system starts automatically each day in the afternoon. The hardware status is checked and initialized, and the observations for the night are scheduled according to all the active request files. The bias, dark current, and twilight flatfield images are automatically taken, and observations of the arranged targets begin when the Sun is 8° below the horizon. A focusing routine is run every 90 min to ensure good focus. During bad weather, such as high winds, high humidity, fog, rain, or completely overcast skies, the slit is closed automatically, and the system takes a “nap” for 10 min. It tries to do observations again after the nap, and keeps trying every 10 min thereafter. At the end of the night the system is shut down automatically; it then goes to “sleep” until waking up again in the afternoon.

The primary science project carried out with KAIT is the Lick Observatory Supernova Search (LOSS; e.g., Treffers et al. 1997; Filippenko et al. 2001), which recently became part of the Lick Observatory and Tenagra Observatory Supernova Searches (LOTOSS; e.g., Schwartz et al. 2000). Depending on the season, about 5,000–10,000 nearby galaxies are monitored every 2 to 15 days by LOSS; over the course of the year, the sample size is about 14,000 galaxies. Images are automatically processed and candidate supernovae (SNe) are flagged; these are subsequently examined by a group of research assistants (most of whom are undergraduate students). Promising SN candidates are then reobserved, and the confirmed SNe are reported to the Central Bureau of Astronomical Telegrams, where the

International Astronomical Union Circulars are issued.

LOSS is the world's most successful search engine for nearby SNe, discovering 20 in 1998, 40 in 1999, 36 in 2000, 68 in 2001, and 82 in 2002. Moreover, most of the LOSS SNe were discovered while young and thus were especially suitable for detailed photometric and spectroscopic studies. The large number of SN discoveries is also ideal for statistical studies such as the SN rate in galaxies of different Hubble types; see van den Bergh, Li, & Filippenko (2002) for the first step of this process, morphological classification of the host galaxies. For more details on the publications utilizing LOSS data, see the web site <http://astron.berkeley.edu/~bait/kait.html> and Filippenko et al. (2003, in preparation).

2.2. The GRB OA Observation Program

Because KAIT does all observations robotically, many years ago we considered incorporating a GRB OA observation program into the system, but the idea was not implemented until the launch of HETE-2. Before HETE-2, the only prompt localizations available were from BATSE; with large positional uncertainties ($\sim 1^\circ - 10^\circ$; Briggs et al. 1999), however, it was impractical to implement a real-time strategy with KAIT (FOV only $6'.7 \times 6'.7$). With the launch of HETE-2, which is capable of providing nearly real-time GRB localization through GCN alerts and significantly improved GRB position uncertainty (about $20' - 40'$, sometimes better than $10'$), the chance of detecting GRB OAs in the small FOV of KAIT has dramatically improved. We thus designed a GRB OA observation program in late 2001, and the system has been operating since the beginning of the year 2002.

The GRB OA observation program connects to the GCN through socket communications, the fastest way (nearly real-time) to receive GRB alerts. Upon receiving a GRB alert, the program responds differently depending on the contents of the alert. If there is no information on the GRB position, or the alert indicates that the trigger was not due to a GRB, only an email message is sent to several team members. When there are GRB coordinates in the alert, and there is no indication that the trigger was not

due to a GRB, the program checks the possibility of observing the GRB field, including the following:

1. The position uncertainty. If the uncertainty exceeds 1° , the field will not be observed.
2. The angular distance from the Moon. Depending on the phase of the Moon, GRB fields within different distances (e.g., 45° during full moon and 25° during quarter moon) from the Moon are not observed.
3. The time of the trigger. If the altitude of the Sun is $< 8^\circ$ below the horizon, it is considered twilight or daytime and the field will not be observed.
4. The telescope limit. Fields that have declination south of -29° or north of $+70^\circ$, or absolute hour angle exceeding 4.5 hr, are not observed due to the mechanical limits of KAIT. As HETE-2 GRBs are preferentially anti-solar, those that are triggered during nighttime hours in California are likely to be within (or close to) the KAIT mechanical limits, except during the summer months.

If the field is determined to be not observable for any reason, an email message is sent to the team members, and the telescope resumes its normal program (usually the SN search), of course continuing to be alert for the next GRB trigger. If, on the other hand, the field can be observed right away, the program immediately terminates the on-going observation by KAIT, and interrupts the previous robotically scheduled observing process.¹ The program then takes a sequence of images of the GRB field, after which the normal automatic observing process resumes.

Thus far, we have chosen to conduct the GRB observations without filters (i.e., in the unfiltered mode). The advantage of this is that deeper limiting magnitudes can be achieved

¹Currently, KAIT cannot stop an exposure in progress, so the shutter remains open during the move to the GRB position. This may even result in a double exposure, of two different parts of the sky, as was the case for GRB 021211 (Li et al. 2003).

in relatively shorter exposures: the limiting magnitude of a 20 s unfiltered exposure is 19.0 (3σ) under favorable observing conditions, while that of a 300 s exposure is 21.5. However, there are two disadvantages to this choice. First, it is difficult to compare unfiltered magnitudes from different telescopes — but as we show in §3, unfiltered photometry can be transferred to the standard Cousins R band with a relatively large color term, and the resulting R magnitudes have uncertainties of about 5%. Second, the unfiltered observation lacks the critical color information to place physical constraints on GRB models — but observations of GRB afterglows are still at a stage where only a few very early (within ten minutes of the burst) light curves have been obtained, and our current goal is to expand the sample with more high-quality early unfiltered light curves. We plan to switch to observing with standard filters in the future.

Our original sequence of observations (before 2002 Nov. 22; UT dates are used throughout this paper) for each GRB field was arranged as follows. First, five 3×20 s grid images (discussed below) were taken, then two 60 s exposures, one 120 s guided exposure, one 300 s guided exposure, and finally, four 120 s guided exposures that combine to make a 2×2 mosaic image centered on the GRB position, covering a region about $12'.7 \times 12'.7$. The whole sequence took about half an hour to observe. The sequence was arranged so that relatively short exposures were observed at the beginning when the GRB OA is expected to be bright, and longer exposures were observed at the end when the OA is expected to become more faint. The 2×2 mosaic observations increased the coverage of the GRB field, but no attempt was made to cover the whole error box of each GRB.

The ROTSE observations of GRB 990123 (Akerlof et al. 1999) have the earliest detection of a GRB OA, and indicate that the early-time light curve of an OA can vary on short timescales: the OA of GRB 990123 brightened by 3 mag in 25 s, then declined by 1 mag in another 25 s. It is important to have good temporal coverage to study these short timescale variations. For this reason, we have developed a procedure to obtain grid images of a GRB field without reading out the CCD. When the first 20 s exposure is finished, the telescope is offset to the east by $0'.6$ (45 pixels), and the CCD shutter is closed but the CCD is not read out. This repeats twice to produce a 3×20 s grid, and the whole image is

finally read out. Although the readout time for the KAIT CCD camera is relatively short (10 s), by saving two readouts the observation efficiency is increased by about 20%, which is significant for the time-critical early OA observations.

The grid procedure adds difficulties to the identification and photometry of individual stars in the final image. However, the offset between the individual 20 s exposures (45 pixels) is big enough to not complicate the photometric reductions too much, and the normal images obtained after the grid procedures offer references to identify individual stars in the grid. There is also the probability that the GRB OA will be superimposed on another star in one or more of the dithering positions, but since the grid images are intended to target bright GRB OAs, the point-spread-function (PSF) fitting procedure in the photometry packages helps determine the individual brightness of the star and the OA. Figure 1 shows a grid image of the GRB 020813 field taken by the KAIT GRB observation program. The GRB OA is marginally detected in each 20 s exposure (see §3 for more details on the observations of GRB 020813). For comparison, Figure 2 shows a non-grid image of the GRB 020813 field.

After the sequence of images of a GRB field is observed, an email message is sent to the team members.² Those who are aware of the observations will then check the data, identify possible OAs and alert the GRB community, and arrange further observations. If no real-time analysis is done, the images are checked the next day by one or more of the team members.

The requested sequence of images has recently been modified, as we learn from our previous attempts to observe GRB OAs. The observations of GRB 020813 showed that the grid images at the beginning of the sequence were not deep enough to detect the GRB OA, and since most GCN alerts with initial positions of GRBs are later than one hour after the bursts, we changed the sequence to start with a relatively shallow (10 s) and a relatively deep (40 s) exposure, followed by a set of grid images. This latter sequence was

²Recently, we modified the system so that a team member is woken up, when there is a particularly promising GRB alert.

followed for GRB 021211, our most successful set of observations of a GRB OA (see next section for details), which demonstrates that grid images are, in fact, effective when GRB positions are determined in real time by HETE-2. Our current (April 2003) sequence thus *starts* with the grid images (first 3×5 s, then 3×10 s and 3×20 s), and continues with longer unguided (60 s) and guided (120 s and 300 s) exposures. We expect the sequence to continue to evolve, reflecting our strategy for observing GRB OAs.

The GRB alert program has also been modified so that incoming GCN notices are studied to determine whether they are first-time alerts, or follow-up alerts of a previous GRB. In the latter case, a different sequence starting with long exposures commences, since the GRB OA is likely to have already faded considerably.

2.3. The System Performance

The KAIT GRB alert program has been in operation since late-December 2001. Our statistics show that during the year 2002, a successful connection was made between KAIT and GCN only 70% of the time. The cause of the connection failures is unknown, but is probably related to network problems. The connectivity has improved to over 90% of the time since November 2002.

Table 1 shows some HETE-2 alerts that KAIT received, but failed to conduct real-time observations for various reasons in 2002. Apparently, most of the failures were caused by bursts occurring during the daytime at KAIT. The only solution to this problem is to have a network of robotic telescopes at different longitudes. Other reasons for failures were bad weather, the connection problem mentioned above, and bursts occurring near or beyond the mechanical or software limits of KAIT. In particular, the HETE-2 on-board localization was derived for GRB 021004 almost immediately, and the GCN alert arrived at KAIT when the GRB was at a western hour angle of 4.4 hr, which is within the mechanical limit of KAIT (4.6 hr), but the software had limited the observations to hour angles within ± 4 hr. We subsequently changed the software limit to ± 4.5 hr, in order to maximize the area of sky potentially accessible to KAIT.

Table 2 shows the HETE-2 alerts that KAIT received and responded to in real time. For the discussions in this paper, $t = 0$ is defined as the GRB on-board trigger time. The position of GRB 020813 was released in a GCN notice at $t = 4.2$ min when it was still daytime at KAIT. We commenced remote manual observations of the GRB field when it was dark ($t = 103.7$ min), but this was interrupted by the KAIT GRB alert program when it received an updated notice at $t = 112.7$ min. KAIT finished a sequence of images of the GRB 020813 field, and then resumed its regular observing schedule. A third GCN notice was received at $t = 184.3$ min, and KAIT responded with the same sequence of images. Using robotic images from the Palomar 48-inch telescope, Fox, Blake, & Price (2002) discovered the OA of GRB 020813. Our manual and automatic observations had successfully imaged this OA position, but not all images are deep enough to detect the OA. We also remotely (but manually) obtained images of the GRB 020813 field the next night. Preliminary results from these observations were reported by Li, Filippenko, & Chornock (2002) and by Li, Chornock, & Filippenko (2002); a detailed analysis is presented in §3.

The GCN alerts with positions for GRB 021104, GRB 021112, and GRB 021113 were received when KAIT was conducting its regular SN search, and the GRB alert program successfully responded with sequences of images. Unfortunately, no OA was discovered for these GRBs from our images, or from images obtained elsewhere.

GRB 021211 is KAIT’s most successfully observed GRB OA. The position of GRB 021211 was relayed by HETE-2 at $t = 22$ s. KAIT responded to the GCN notice at $t = 32$ s, and began to slew across much of the sky to the GRB position. It finished pointing at $t = 108$ s (but the dome slit began to clear the telescope at $t = 105$ s), with 48 s left in a 600 s follow-up exposure of SN 2002he. Because currently we cannot stop an exposure in progress, the image ended up with the GRB 021211 field superimposed on the SN 2002he field (but nevertheless a useful image which provided the earliest KAIT measurement of GRB 021211). KAIT then took a sequence of images, starting with a 10 s exposure and continuing with exposures of 40 s, 3×20 s grid, 60 s, 120 s (guided), and 300 s (guided). Three additional GCN alerts with updated positions for GRB 021211 were received during the night, and KAIT responded with the same sequence of images. The position of the OA

of GRB 021211 (Fox & Price 2002) was successfully observed on most images. Preliminary results from these observations were reported by Li et al. (2002) and Chornock et al. (2002), and a detailed analysis is presented elsewhere (Li et al. 2003). Our observations of GRB 021211 not only provide one of the fastest detections of a GRB OA, but also show evidence for a reverse-shock component in the early optical emission and a break at $t \approx 10$ min. Our photometry of GRB 021211, which has high temporal resolution, also suggests that either the object underwent a dramatic color change at early times, or that there are small-scale variations superimposed on the power-law decay of the reverse-shock emission (Li et al. 2003).

The experience we gained from the observations of the GRB 021211 OA prompted us to make improvements to the existing GRB alert program. For example, the response procedure was simplified to speed up the observations, the sequence of images was changed to start with short 3×5 s grid images, and follow-up GCN alerts are observed with a sequence starting with relatively long exposures instead of short ones.

Table 2 also shows that KAIT can typically start the first observation at about 20–40 s after receiving the GCN alert. With our improved procedure, tests show that KAIT can start the first exposure as early as 8 s after receiving a position from the GCN notices. Table 2 also shows that with small-number statistics, KAIT is more successful with GRBs that have near real-time HETE-2 localizations (e.g., GRB 020813 and GRB 021211) than with GRBs that are localized more than 600 s after the bursts.

3. OBSERVATIONS OF GRB 020813

3.1. Data Reduction

GRB 020813 was detected by HETE-2 at 2:44 on 2002 August 13 (Villasenor et al. 2002). The gamma-ray light curve shows a series of pulses that last > 125 s, typical of a bright, long-duration burst. The flight localization was reported in a GCN notice at $t = 4.2$ min. The OA of GRB 020813 was discovered by Fox, Blake, & Price (2002) in images taken

at $t \approx 2$ hr with the Palomar 1.2 m Oschin Schmidt telescope; independent analysis of our own images also revealed the OA (Li, Chornock, & Filippenko 2002), but we reported the results later than Fox, Blake, & Price (2002). Spectroscopy of the GRB 020813 OA with the Keck telescope (Price et al. 2002) identifies absorption systems with the highest redshift measured at $z = 1.254$. Spectropolarimetric observations also done with Keck (Barth et al. 2002, 2003) yield a linear polarization of 1.8–2.4% at $t = 4.7$ – 4.9 hr, the first spectropolarimetry ever obtained for a GRB OA. A temporal break in the light curve was first suggested by Bloom, Fox, & Hunt (2002), and confirmed by us (Li, Chornock, & Filippenko 2002), Malesani et al. (2002), and Gladders & Hall (2002b).

We obtained 25 images of the GRB 020813 field on 2002 August 13, among which 9 were manually and 16 were automatically observed. A total of 45 individual exposures of the GRB 020813 OA were taken due to our grid procedure. An additional 6 images were manually taken on 2002 August 14. Because of the faintness and the rapid decline of the OA, not all of our images are useful.

Since our observations were obtained without filters, it is important to transform the measured magnitudes to a standard photometric system, so that comparisons with observations taken elsewhere can be made. In reducing unfiltered data on Type Ia SNe, Riess et al. (1999) demonstrated a method that treats the unfiltered images as though they were observed through a very broad filter, and uses color terms to correct for the difference in the throughput curves, just as we correct the instrumental *BVRI* magnitudes to the standard Johnson-Cousins system. The color terms can be empirically determined by obtaining *BVRI* and unfiltered images of Landolt (1992) standard stars during photometric nights. Riess et al. found that for a SN Ia, whose spectrum has broad absorption and emission features and is far from stellar, a reliable transformation from unfiltered magnitudes to a standard passband can be achieved at a precision of $\sim 5\%$. Since most GRB OA spectra don't have broad absorption and emission features, we expect the transformation to work even better for the unfiltered GRB OA observations.

We find that the combination of the KAIT optics and the quantum efficiency of the Apogee CCD camera makes the KAIT unfiltered observations mostly mimic the *R* band, so

we choose to transform the unfiltered magnitudes to R . The formula for the differential photometry that transforms the unfiltered magnitudes to R is as follows:

$$R_{GRB} = (c_{GRB} - c_{LS}) + R_{LS} - CT \times [(V - R)_{GRB} - (V - R)_{LS}], \quad (1)$$

where R_{GRB} , c_{GRB} , and $(V - R)_{GRB}$ are the R magnitude, unfiltered magnitude, and $(V - R)$ color of the GRB OA, respectively, while R_{LS} , c_{LS} , and $(V - R)_{LS}$ are those of the local standard star. “ CT ” is the color term to transform the KAIT unfiltered magnitudes to R , and is found to be 0.27 ± 0.05 from several photometric nights.

We have adopted the calibration of the GRB 020813 field by Henden (2002), and $(V - R) = 0.39$ mag for GRB 020813 from Gladders & Hall (2002a). The final transformed R magnitudes from the unfiltered KAIT observations are listed in Table 3.

To cross-check the accuracy of the above transformation, we have independently measured the extensive R -band photometry of the GRB 020813 OA by the 6.5-m Magellan telescope, which were generously made available to the GRB community by Gladders & Hall (2002c). The same calibration of the GRB 020813 field (Henden 2002) was used. The measured R magnitudes are listed in Table 4.

Figure 3 displays the R -band light curve of the GRB 020813 OA from the unfiltered KAIT observations, while Figure 4 shows that from KAIT, Magellan, the BAO 1.0-m telescope (Kawabata, Urata, & Yamaoka 2002), and the TUG 1.5-m (Kiziloglu et al. 2002) observations. In these figures we assume no host-galaxy reddening to GRB 020813 (Barth et al. 2003), and adopt a Galactic extinction of $A_R = 0.26$ mag (Schlegel, Finkbeiner, & Davis 1998). It is apparent from both figures that there is a break in the light curve of the GRB 020813 OA at $t \approx 0.2$ d, which is further qualitatively demonstrated by the change of power-law decay indices before and after the break: -0.47 ± 0.04 at $t = 0.0720$ – 0.1363 d from the KAIT observations, and -1.16 ± 0.04 at $t = 0.2336$ – 1.1873 d from the KAIT observations (-1.08 ± 0.03 from all the observations shown in Figure 4). The break appears to be smooth and gradual. For example, the power-law decay index measured at $t = 0.1334$ – 0.2357 d is -0.81 ± 0.06 from the KAIT observations (-0.83 ± 0.05 from all the

observations shown in Figure 4), which is in between the earlier and later power-law decay indices.

To better describe the temporal evolution of the GRB 020813 OA, we fit the data with a smoothly broken power-law model, which is modified from that of Beuermann et al. (1999):

$$F_\nu = \frac{2^{1/s} F_{\nu,b}}{[(t/t_b)^{-\alpha_1 s} + (t/t_b)^{-\alpha_2 s}]^{1/s}}, \quad (2)$$

where t_b is the time of the break, $F_{\nu,b}$ is the flux at t_b , and s controls the sharpness of the break, with larger s implying a sharper break. We obtained the following values for the parameters using a χ^2 -minimizing procedure: (1) for the KAIT data only: $t_b = 0.14 \pm 0.03$ day, $\alpha_1 = -0.13 \pm 0.05$, $\alpha_2 = -1.21 \pm 0.12$, and $s = 2.2 \pm 0.8$. The reduced χ^2 of the fit is 1.12 for 13 degrees of freedom. (2) For all the data shown in Figure 4: $t_b = 0.13 \pm 0.03$ day, $\alpha_1 = -0.21 \pm 0.05$, $\alpha_2 = -1.09 \pm 0.08$, and $s = 3.3 \pm 1.0$. The reduced χ^2 of the fit is 0.63 for 29 degrees of freedom. The dashed lines in the upper panels of Figures 3 and 4 show the model fits, while the lower panels of the two figures show the residuals of the fits.

The reduced χ^2 values of both fits show that eq. (1) is an adequate model to fit the data. The derived parameters from both fits are consistent with each other within the uncertainties, indicating that the transformed KAIT R data are consistent with the other R -band measurements. In particular, the superb Magellan data offer a good consistency check, and it can be seen from both the model fit (upper panel of Figure 4) and the residual of the fit (lower panel of Figure 4) that the KAIT data are consistent (± 0.05 mag) with those of Magellan, although with much bigger uncertainties.

Our reduction of the KAIT data thus confirms the results of Riess et al. (1999) that the unfiltered magnitudes can be reliably transformed to a standard passband with a precision of $\sim 5\%$, given that the color term is well determined and the color of the target is known. The high throughput of the unfiltered observations thus provides a unique way to go deep for small to moderate telescopes, while still providing reasonably accurate photometry in a passband close to the peak of the unfiltered response function.

However, we need to also emphasize the limitations of this transformation. An *a priori* requirement for the transformation is that the color of the OA is known at the time of the unfiltered observations, which is often *not* the case. For example, we assumed that the color of the GRB 020813 OA is constant at all of the epochs of the KAIT unfiltered observations, and is the same as reported by Gladders & Hall (2002a) at times that are only coincident with the second part of the KAIT observations. Early GRB OAs are expected to have a large blue to red evolution (Sari, Piran, & Narayan 1998), though this has not yet been confirmed with observations, probably because most of the filtered observations commenced too late. Clearly, the poor constraints on the color evolution of GRB OAs is the main impediment to transforming unfiltered magnitudes to a standard passband. Nevertheless, to expedite comparisons between unfiltered observations from different observatories, it is important to apply such a transformation and provide information such as the color term and the color used in the transformation, so that other observers can correct the reported photometry with different color estimates. For example, if the $(V - R)$ color of the GRB 020813 OA is assumed to be VR , the photometry reported in Table 3 will need to be increased by $0.27 \times (0.39 - VR)$ mag.

3.2. Late-Time Power-Law Decay Index and Spectral Index

Although the power-law decay index after the break (α_2) for the GRB 020813 OA is measured to be -1.09 ± 0.08 from the model fit to all the data shown in Figure 4 as discussed above, later observations in the optical (Malesani et al. 2002; Levan et al. 2002) and X-rays (Vanderspek et al. 2002) indicate a further steepening of the light curve. This suggests that the GRB 020813 OA has a smoothly changing light curve, as partly demonstrated by the data shown in Figure 4; it also suggests that our measured value of α_2 is only an intermediate result between the early and the late-time measurements, and that the derived parameters $(t_b, \alpha_1, \alpha_2, s)$ may need to be revised when later data are considered in the model fit. Unfortunately, such late-time data for GRB 020813 are not available at the time of writing; thus, we adopt $\alpha_2 = -1.39 \pm 0.05$, which is the average of values reported by Malesani et al. (2002), Levan et al. (2002), and Vanderspek et al.

(2002). The power-law decay index before the break (α_1) is not expected to be significantly changed, as it is dominated by the early-time measurements already presented here, so we adopt $\alpha_1 = -0.21 \pm 0.05$ from the model fit to all the data shown in Figure 4.

The optical spectral index of the GRB 020813 OA was reported as $\beta = -1.06 \pm 0.01$ from red-channel Keck spectra (5600–9400 Å) taken at $t \approx 6$ hr (Barth et al. 2003). Levan et al. (2002) reported a shallower optical spectral index of $\beta = -0.8$ from *Hubble Space Telescope* images taken at $t \approx 98$ hr after the burst. We adopt the Keck measurement, as it was made during the time of the photometric observations presented here, and we correct it for a Galactic reddening of $E(B - V) = 0.11$ mag (Schlegel, Finkbeiner, & Davis 1998). The final β we use for the GRB 020813 OA is -0.73 ± 0.01 .

3.3. Discussion

The current standard model for GRBs and their afterglows is the fireball shock model (for a review see Mészáros 2002), in which a fireball expands relativistically into an ambient medium and decelerates as it sweeps up matter. The shock between the fireball and the medium accelerates electrons to relativistic energies, and gives them a power-law differential energy distribution with index $-p$. The simplest afterglow model (e.g., Sari, Piran, & Narayan 1998) predicts that the afterglow flux $f_\nu(t) \propto t^\alpha \nu^\beta$, where $f_\nu(t)$ is the flux at frequency ν , and β is the spectral index of the OA. Interpretation of the afterglow data in the framework of these models can, in principle, yield many interesting parameters of the GRB explosion (e.g., Wijers, Vreeswijk, & Galama 1999; Holland et al. 2000) because the properties of the observed light curve of the afterglow, such as the power-law decay rate α , are primarily determined by the hydrodynamic evolution (e.g., adiabatic or radiative), the geometry (spherical or collimated), and the density profile of the ambient medium (constant or stellar-wind type) of the fireball (e.g., Sari, Piran, & Narayan 1998; Wijers & Galama 1998; Rhoads 1999; Chevalier & Li 2000).

A break in the OA light curve is often regarded as a signature of a jet (e.g., Mészáros & Rees 2000; Kulkarni et al. 1999; Rhoads 1999; Moderski, Sikora, & Bulik 2000), either

with a fixed opening angle θ_0 , or expanding sideways as well as radially. A jet with a fixed opening angle θ_0 can have a break in the light curve when the Lorentz factor decreases to $\sim 1/\theta_0$, due to the geometrical effect that the observer only receives radiation emitted within the collimated beam. A jet that expands sideways as well as radially can have a break in the light curve when the sideways expansion dominates over the radial expansion.

During the initial phase, however, the GRB outflow looks spherical to the observer in most current models. Under the assumptions of adiabatic cooling and an ambient medium of constant density, the predicted power-law decay index in this phase is $\alpha_1 = -(3p - 3)/4$, when $\nu < \nu_c$ (the cooling frequency, above which the electrons cool on the dynamical timescale of the system), and $\alpha_1 = -(3p - 2)/4$ when $\nu > \nu_c$ (e.g., Sari, Piran, & Halpern 1999). The measured $\alpha_1 = -0.21 \pm 0.05$ then implies $p = 1.28$ ($\nu < \nu_c$), or $p = 0.95$ ($\nu > \nu_c$), which would imply a diverging electron energy. This may be an indication that (1) radiative process may be significant, though Sari, Piran, & Narayan (1998) show that a radiative fireball decays with $\alpha_1 = -4/7$, which is still steeper than the observations; (2) the ambient medium may not have a constant density — for an outflow expanding into a stellar wind environment, Chevalier & Li (2000) calculate $\alpha_1 = -1/4$ at early times of a GRB when $\nu > \nu_m$ (the peak frequency, which corresponds to the minimum-energy electrons), in good agreement with the observations; (3) energy is being injected into the outflow even during the afterglow phase (e.g., Zhang & Mészáros 2002), a hypothesis that could be constrained with radio and X-ray observations; or (4) there is a significant color change for the early afterglow, so that the transformation from the unfiltered magnitudes to R is incorrect. However, to achieve a steeper α_1 , the color of the afterglow will need to change from red to blue, inconsistent with the model prediction by Sari, Piran, & Narayan (1998). Alternatively, there are some theoretical considerations (e.g., Bykov & Mészáros 1996) to allow the formation of a flat electron spectrum (i.e., $p < 2$).

GRB 020813 has the slowest pre-break decline rate, α_1 , of all GRBs with well measured optical light-curve breaks (which all show $\alpha_1 \lesssim -0.7$; see, e.g., Figure 3 of Stanek et al. 2001). Afterglow models generally predict a correlation between the decline rates α and the spectral index β ; for GRB 020813, however, the observed $\beta = -0.73$ is fairly typical among

GRB OAs. To be more consistent with the models, it is possible to invoke host-galaxy extinction; as little as $E(B - V) = 0.05$ mag of reddening in the host would imply an intrinsic $\beta = -0.50 \pm 0.03$, which increases to $\beta = -0.26 \pm 0.03$ for $E(B - V)_{\text{host}} = 0.10$ mag. However, such flat spectral indices typically imply unreasonable electron indices $p \lesssim 1$, and thus host-galaxy extinction is unlikely to explain the peculiarities of GRB 020813.

The amplitude of the break ($\Delta\alpha = \alpha_2 - \alpha_1$) is independent of extinction with the assumption of no color change, and can also be used to constrain models. For GRB 020813, we find $\Delta\alpha = -1.18 \pm 0.07$, which is also fairly typical among well-observed GRBs. In the framework of a constant ambient density model, this result favors a sideways-expanding jet ($\Delta\alpha = \alpha_1/3 - 1 = -1.07 \pm 0.02$) over a jet with a fixed opening angle ($\Delta\alpha = -3/4$; Rhoads 1999), but as discussed above, a wind medium may better explain the early decline.

4. CONCLUSIONS

In this paper we present the technical details of the GRB alert system at KAIT, a 0.76 m telescope with relatively high resolution imaging capacity ($0''.8 \text{ pixel}^{-1}$). Connected to the GCN via socket communication, KAIT is capable of responding to GRB alerts in real time, and of capturing a pre-arranged sequence of images automatically. The observations are done in the unfiltered mode to reach deeper limiting magnitudes in relatively shorter exposures. A grid image procedure is used to increase the efficiency of the early-time observations. The sequence of images starts with short-exposure grid images, and continues with increasingly longer exposures to compensate for the decline of a GRB OA. A different sequence that starts with long exposures is followed in response to a GCN notice with updated positions for a previous GRB. All of these efforts are aimed to getting good early-time photometry rather than searching wide regions for the OAs of GRBs.

Our reduction of the GRB 020813 data taken with KAIT shows that unfiltered magnitudes can be reliably transformed to a standard passband with a precision of $\sim 5\%$, if the color of the object is known.

The available data on GRB 020813 from KAIT, Magellan, and elsewhere (as reported in the GCN Circulars) indicate that the GRB 020813 OA has an exceptionally slow early-time power-law decay index, though other light-curve parameters and the optical spectral index are fairly typical. GRB 020813 thus presents an interesting challenge to afterglow models for GRBs; additional observations (for instance, in the radio or X-rays) may shed light on the situation for this particular burst. Continued automatic observations with KAIT of other bursts in the future will help determine whether GRB 020813 remains exceptional in a larger sample.

A.V.F. is grateful to Stan Woosley for encouraging him, years ago, to use KAIT for the optical follow-up of GRBs having sufficiently precise coordinates. We thank Mike Gladders and Pat Hall for making their superb Magellan data available and for assistance with the reductions, and Scott Barthelmy for his help setting up the KAIT GRB alert system. We also thank Shiho Kobayashi and Bing Zhang for useful discussions. The work of A.V.F.'s group at U. C. Berkeley is supported by National Science Foundation grant AST-9987438, as well as by the Sylvia and Jim Katzman Foundation. KAIT was made possible by generous donations from Sun Microsystems, Inc., the Hewlett-Packard Company, AutoScope Corporation, Lick Observatory, the National Science Foundation, the University of California, and the Katzman Foundation. S.J. thanks the Miller Institute for Basic Research in Science at U. C. Berkeley for support through a research fellowship.

Table 1. KAIT Responses to HETE-2 Alerts in 2002; No Real-Time Observations^a

Trig.	UT date (yy/mm/dd)	UT time (hh:mm:ss)	Δt^b (min)	α_{J2000} (d eg.)	δ_{J2000} (deg.)	Err. ^c	OA ^d	Reason ^e
1896	02/01/24	10:41:15.13	85.6	143.206	−11.460	24′	yes	bad weather
1902	02/01/27	20:57:24.73	105.6	123.774	+36.742	24′	no	daytime
1939	02/03/05	11:55:25.05	596.5	190.762	−14.552	50′	yes	daytime
1959	02/03/17	18:15:31.42	533.6	155.837	+12.744	36′	no	bad weather
1963	02/03/31	16:32:28.76	40.4	199.142	−17.875	20′	yes	daytime
2042	02/05/31	00:26:18.71	88.0	228.688	−19.360	77′	no	daytime ^f
2081	02/06/25	11:25:49.32	173.6	311.060	+07.170	28′	no	daytime
2257	02/08/12	10:41:43.98	9.1	309.699	−05.393	28′	no	no connection
2262	02/08/13	02:44:19.16	6.5	296.658	−19.588	2′	yes	daytime ^g
2275	02/08/19	14:57:35.82	98.1	351.849	+6.269	4′	no	daytime
2380	02/10/04	12:06:13.57	0.8	6.737	+18.929	4′	yes	telescope limit ^h
2397	02/10/16	10:29:00.74	104.2	2.768	+49.139	659′	no	telescope limit

^aOnly alerts with position information are listed.

^bThe time delay (minutes) between the GRB trigger and the first reported GCN position.

^cThe uncertainty of the given position (diameter).

^dWhether an OA was detected by us or by others.

^eThe reason why no KAIT real-time observations were made.

^fThe GRB was manually observed later, and the results were reported by Li, Chornock, & Filippenko (2002).

^gThe GRB was manually and automatically observed later. See text for details.

^hThe GRB was initially within KAIT’s mechanical limit, but not within its software limit; see text for details.

Table 2. KAIT Responses to HETE-2 alerts in 2002; Real-Time Observations

Trig.	UT date (yy/mm/dd)	UT time (hh:mm:ss)	Δt^a (min)	Obs(t) ^b (min)	α_{J2000} (deg.)	δ_{J2000} (deg.)	Err.	OA	t1 ^c (s)	Exp ^d (s)
2262	02/08/13	02:44:19.16	4.2	112.7	296.658	−19.588	2′	yes	143	3×20
2262	02/08/13	02:44:19.16	4.2	184.3	296.658	−19.588	2′	yes	63	3×20
2434	02/11/04	07:01:02.93	166.0	166.0	58.452	+37.953	52′	no	24	3×20
2448	02/11/12	03:28:15.89	81.2	81.2	39.127	+48.849	40′	no	108	3×20
2448	02/11/12	03:28:15.89	81.2	121.1	39.127	+48.849	40′	no	28	3×20
2449	02/11/13	06:38:56.90	120.9	120.9	23.473	+40.462	27′	no	40	3×20
2449	02/11/13	06:38:56.90	120.9	153.6	23.473	+40.462	27′	no	31	3×20
2493	02/12/11	11:18:34.03	0.4	0.5	122.228	+6.735	28′	yes	108 ^e	10
2493	02/12/11	11:18:34.03	0.4	34.9	122.228	+6.735	28′	yes	35	10
2493	02/12/11	11:18:34.03	0.4	66.8	122.228	+6.735	28′	yes	23	10
2493	02/12/11	11:18:34.03	0.4	131.0	122.250	+6.739	4′	yes	45	10

^aThe time delay (minutes) between the GRB trigger and the first reported GCN position.

^bThe time (minutes after the GRB trigger) of the alert message that activates KAIT.

^cThe response time when KAIT started the first observation.

^dThe exposure time for the first observation.

^eThis image is a superposition of two fields; see text for details. The exposure actually started at $t = 105$ s, when the dome slit began to clear the telescope.

Table 3. KAIT Photometry of the GRB 020813 OA

UT time ^a	t (hr) ^b	Exp. (s)	R^c	σ_R^c	Obs. ^d
4:28:00	1.728	30	17.90	0.05	m
4:28:46	1.740	30	17.98	0.06	m
4:29:32	1.754	30	17.81	0.05	m
4:32:12	1.797	120	17.91	0.04	m
4:36:43	1.874	300	17.94	0.04	m
4:46:11	2.030	30	17.92	0.06	a
4:46:58	2.045	30	17.95	0.07	a
4:50:21	2.100	300	18.00	0.07	a
5:56:28	3.201	30	18.16	0.06	a
5:57:14	3.216	30	18.08	0.05	a
6:00:36	3.271	300	18.23	0.02	a
7:35:18	4.850	120	18.58	0.04	m
7:39:15	4.915	120	18.54	0.05	m
8:20:41	5.606	120	18.73	0.08	m
8:23:45	5.657	300	18.67	0.05	m
5:02:55	26.311	600	20.59	0.18	m
7:00:58	28.277	600	20.77	0.23	m

^aUT time at the middle of the exposure. All are on 2002 August 13, except the last two which were on August 14.

^bStarting time after the GRB, in hours.

^cMagnitude and 1σ uncertainty derived from unfiltered observations; see text for details.

^d“Observer” of the images: those marked with “m” were manually obtained via remote observations; while those marked with “a” were obtained by the automatic GRB alert program.

Table 4. Magellan Photometry of the GRB 020813 OA^a

UT time ^b	t (hr) ^c	R^d	σ_R^d
6:41:52	3.967	18.40	0.03
6:54:14	4.173	18.43	0.02
6:56:02	4.205	18.44	0.02
7:08:22	4.409	18.48	0.03
7:09:52	4.435	18.49	0.02
7:11:22	4.459	18.49	0.02
7:12:52	4.483	18.50	0.02
7:18:50	4.584	18.52	0.03
7:23:03	4.653	18.54	0.03
7:30:00	4.769	18.56	0.03
1:14:11	22.507	20.30	0.03
1:15:41	22.531	20.31	0.03
1:17:11	22.555	20.32	0.03
1:18:41	22.581	20.33	0.03

^aMeasured from the publically available data on site ftp.ociw.edu under pub/gladders/GRB/GRB020813. All exposures were of 60 s duration.

^bUT time at the middle of the exposure. All are on 2002 August 13, except the last four which were on August 14.

^cStarting time after the GRB, in hours.

^d R -band magnitude and 1σ uncertainty.

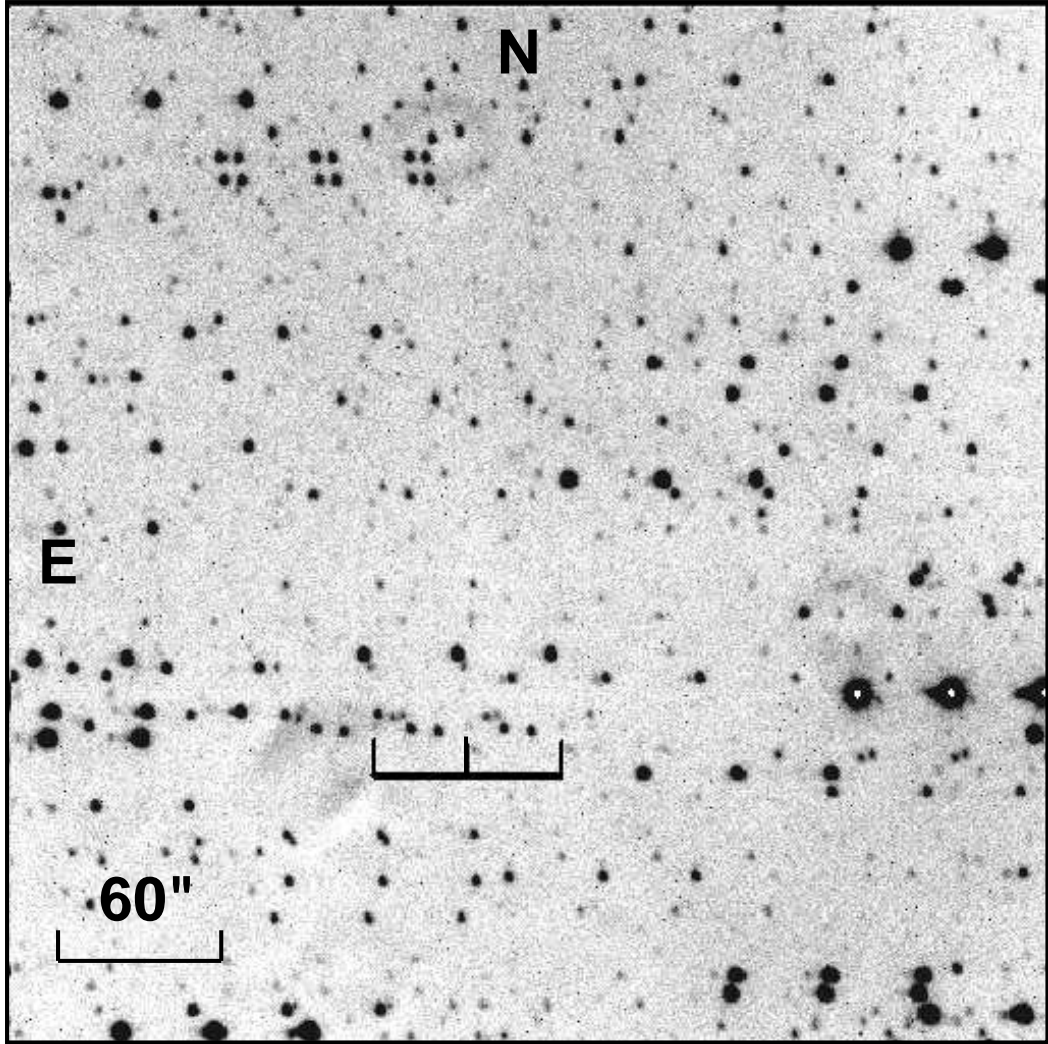


Fig. 1.— An unfiltered KAIT grid image of the GRB 020813 field. The OA of GRB 020813, which is quite faint, is marked at three positions.

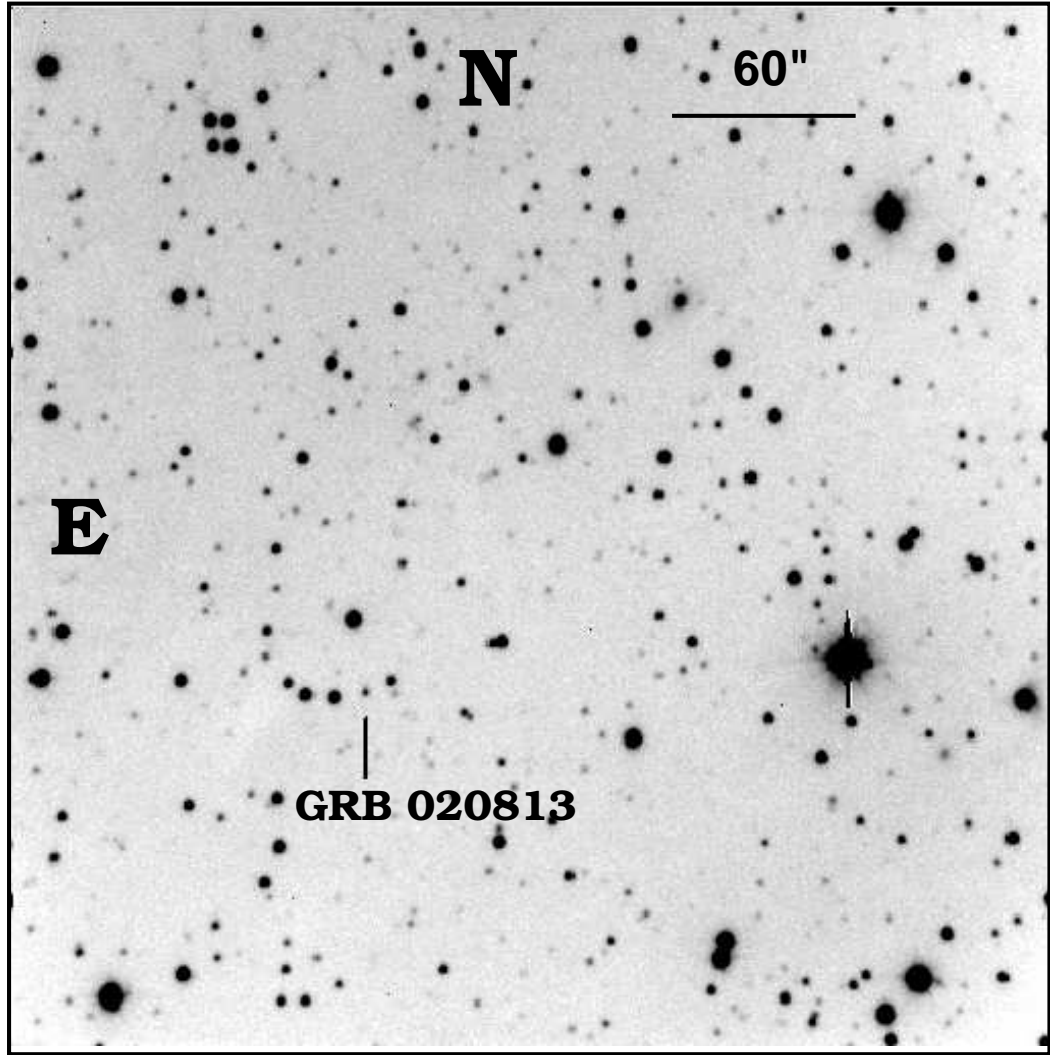


Fig. 2.— An unfiltered KAIT non-grid image of the GRB 020813 field. The OA of GRB 020813 is marked.

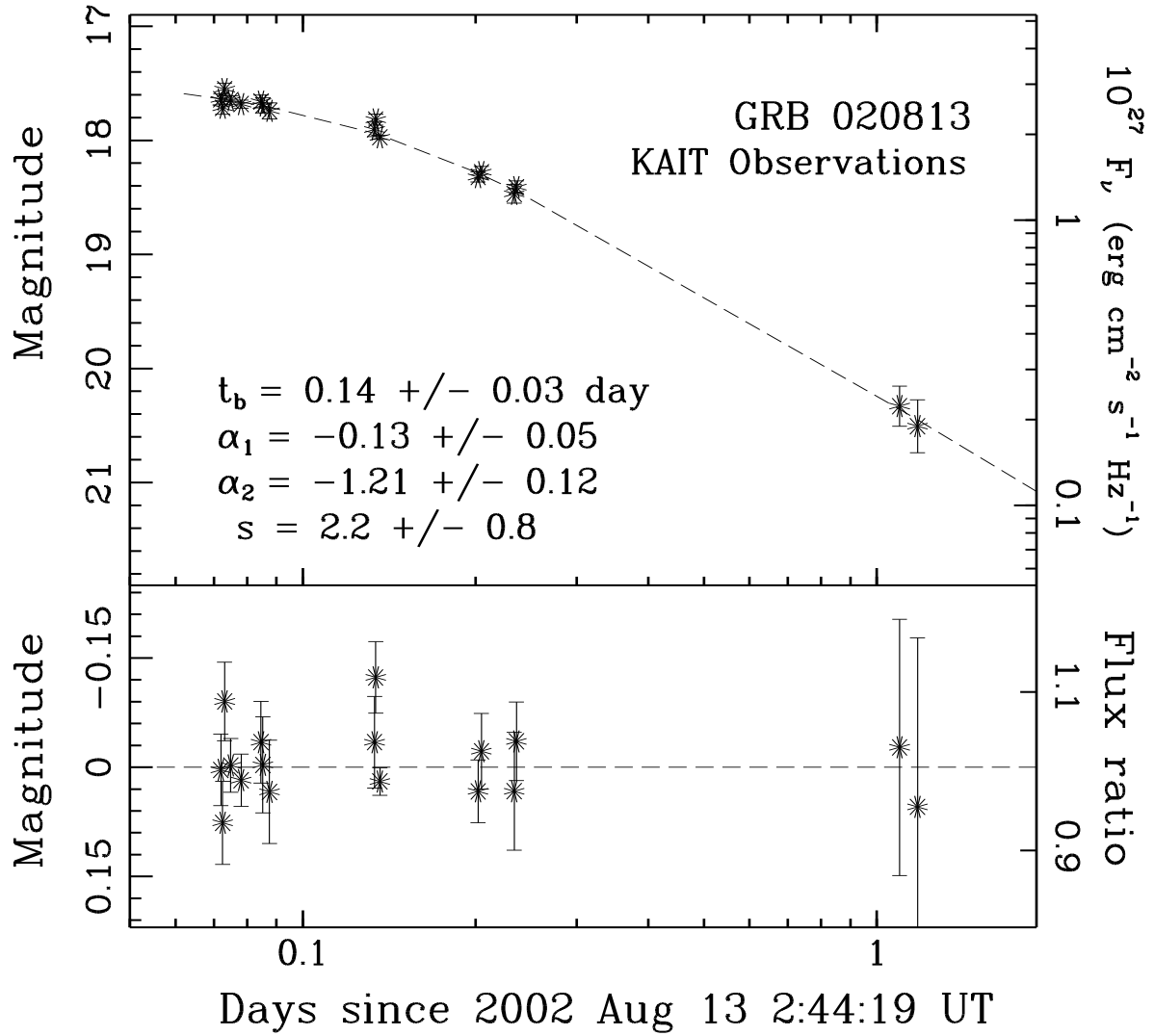


Fig. 3.— Light curve of the GRB 020813 OA from the KAIT observations. The upper panel shows the broken power-law fit, while the lower panel shows the residuals of the fit.

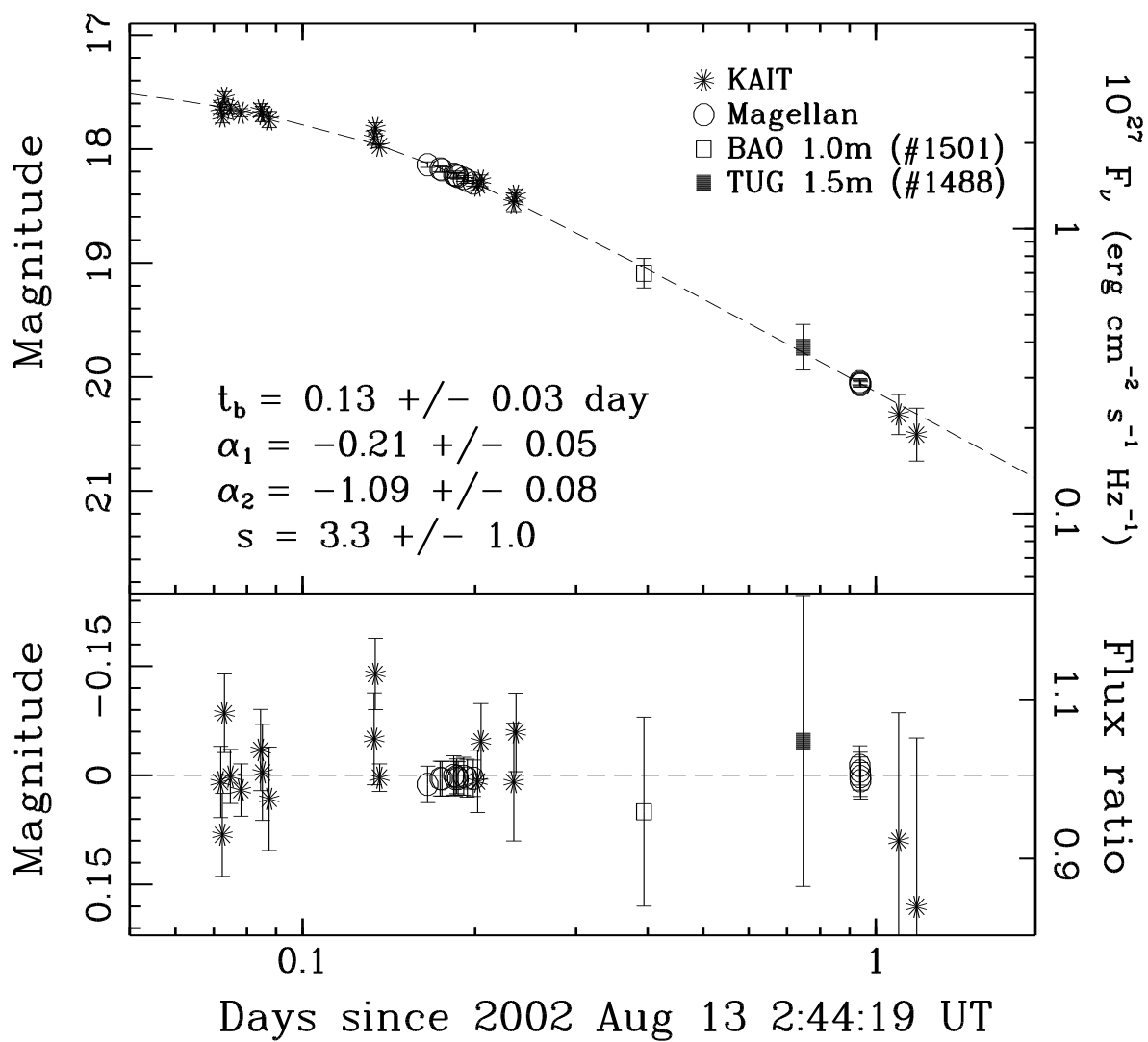


Fig. 4.— Light curve of the GRB 020813 OA from various sources. The upper panel shows the broken power-law fit, while the lower panel shows the residuals of the fit.

REFERENCES

- Akerlof, C. W., & McKay, T. A. 1999, IAU Circ. 7100
- Akerlof, C. W., et al. 1999, *Nature*, 398, 400
- Barth, A. J., Cohen, M. H., Goodrich, R. W., Price, P. A., Bloom, J. S., & Fox, D. W. 2002, GCN Circ. 1477
- Barth, A. J., Sari, R., Cohen, M. H., Goodrich, R. W., Price, P. A., Fox, D. W., Bloom, J. S., Soderberg, A. M., & Kulkarni, S. R. 2003, *ApJ*, 584, L47
- Barthelmy, S. D., et al. 1994, in *Proceeding of the 2nd Huntsville Workshop*, ed. G. Fishman, J. Brainerd, & K. Hurley (New York: AIP), 643
- Beuermann, K., et al. 1999, *A&A*, 352, L26
- Bloom, J. S., Fox, D. W., & Hunt, M. P. 2002, GCN Circ. 1476
- Boella, G., Butler, R. C., Perola, G. C., Piro, L., Scarsi, L., & Bleeker, J. A. M. 1997, *A&AS*, 122, 299
- Briggs, M. S., Pendleton, G. N., Kippen, R. M., Brainerd, J. J., Hurley, K., Connaughton, V., & Meegan, C. A. 1999, *ApJS*, 122, 503
- Bykov, A. M., & Mészáros, P. 1996, *ApJ*, 461, L37
- Chevalier, R. A., & Li, Z.-Y. 2000, *ApJ*, 536, 195
- Chornock, R., Li, W., Filippenko, A. V., & Jha, S. 2002, GCN Circ. 1754
- Filippenko, A. V., Li, W., Treffers, R. R., & Modjaz, M. 2001, in *Small-Telescope Astronomy on Global Scales*, ed. W. P. Chen, et al. (San Francisco: ASP), 121
- Fox, D. W., Blake, C., & Price, P. 2002, GCN Circ. 1470
- Fox, D. W., & Price, P. A. 2002, GCN Circ. 1731

- Gladders, M., & Hall, P. 2002a, GCN Circ. 1513
- Gladders, M., & Hall, P. 2002b, GCN Circ. 1514
- Gladders, M., & Hall, P. 2002c, GCN Circ. 1519
- Henden, A. 2002, GCN Circ. 1503
- Holland, S., Björnsson, B., Hjorth, J., & Thomsen, B. 2000, A&A, 364, 467
- Kawabata, T., Urata, Y., & Yamaoka, H. 2002, GCN Circ. 1501
- Kiziloglu, U., et al. 2002, GCN Circ. 1488
- Kulkarni, S. R., et al. 1999, Nature, 398, 389
- Landolt, A. U. 1992, AJ, 104, 340
- Levan, A. J., Fruchter, A. S., Burud, I., & Rhoads, J. E. 2002, GCN Circ. 1518
- Li, W., Chornock, R., & Filippenko, A. V. 2002, GCN Circ. 1491
- Li, W., Filippenko, A. V., & Chornock, R. 2002, GCN Circ. 1473
- Li, W., Filippenko, A. V., Chornock, R., & Jha, S. 2002, GCN Circ. 1737
- Li, W., Filippenko, A. V., Chornock, R., & Jha, S. 2003, ApJ, 586, L9
- Li, W., et al. 2000, In Cosmic Explosions, ed. S. S. Holt & W. W. Zhang (New York: AIP), 103
- Malesani, D., Covino, S., Fugazza, D., Barrena, R., Pian, E., & Masetti, N. 2002, GCN Circ. 1500
- Meegan, C. A., Fishman, G. J., Wilson, R. B., Paciesas, W. S., Pendleton, G. N., Horack, J. M., Brock, M. N., & Kouveliotou, C. 1992, Nature, 355, 143
- Mészáros, P. 2001, Science, 291, 79

- Mészáros, P. 2002, *ARA&A*, 40, 137
- Mészáros, P., & Rees, M. J. 2000, *ApJ*, 530, 292
- Moderski, R., Sikora, M., & Bulik, T. 2000, *ApJ*, 529, 151
- Park, H. S., et al. 2001, in *Gamma 2001: Gamma-Ray Astrophysics*, ed. S. Ritz, N. Gehrels, & C. R. Shrader (New York: AIP), 181
- Price, P. A., Bloom, J. S., Goodrich, R. W., Barth, A. J., Cohen, M. H., & Fox, D. W 2002, *GCN Circ.* 1475
- Rhoads, J. E. 1999, *ApJ*, 525, 737
- Richmond, M., Treffers, R. R., & Filippenko, A. V. 1993, *PASP*, 105, 1164
- Ricker, G. R., et al. 2001, *BAAS*, 198, 3504
- Riess, A. G., et al. 1999, *AJ*, 118, 2675
- Sari, R., Piran, T., & Halpern, J. P. 1999, *ApJ*, 519, L17
- Sari, R., Piran, T., & Narayan, R. 1998, *ApJ*, 497, L17
- Schlegel, D. J., Finkbeiner, D. P., & Davis, M. 1998, *ApJ*, 500, 525
- Schwartz, M., Li, W., Filippenko, A. V., Modjaz, M., & Treffers, R. R. 2000, *IAU Circ.* 7514
- Stanek, K. Z., et al. 2001, *ApJ*, 563, 592
- Treffers, R. R., Peng, C. Y., Filippenko, A. V., Richmond, M. W., Barth, A. J., & Gilbert, A. M. 1997, *IAU Circ.* 6627
- Treffers, R. R., et al. 1995, In *Robotic Telescopes*, ed. G. W. Henry & J. A. Eaton (San Francisco: ASP), 86
- van den Bergh, S., Li, W., & Filippenko, A. V. 2002, *PASP*, 114, 820

Vanderspek, R., Marshall, H. L., Ford, P. G., & Ricker, G. R. 2002, GCN Circ. 1504

Villasenor, J., et al. 2002, GCN Circ. 1471

Wijers, R. A. M. J., & Galama, T. J. 1998, ApJ, 523, 177

Wijers, R. A. M. J., Vreeswijk, P. M., & Galama, T. J. 1999, ApJ, 523, L33

Zhang, B., & Mészáros, P. 2002, ApJ, 566, 712